

A Planar Delta–Cross Shaped Loop Antenna: Analysis and Simulation – The 2 WL Case

G.A. Papadaniel, N.I. Yannopoulou, P.E. Zimourtopoulos *

[1] Independent Researcher, Thessaloniki, Greece
[2, 3] Antennas Research Group, Hellas – Austria

Abstract

A planar Delta–Cross shaped loop antenna is proposed. The presentation includes results from an analytic study of the radiation pattern, as well as, from a simulation study for both the electric and radiation characteristics: input impedance, standing wave ratio, radiation pattern and directivity. The loop was initially shaped as 4 non-overlapping equilateral triangles on a plane, symmetrically oriented around a common vertex, center fed at one triangle base. In order to improve the antenna characteristics, its shape was then modified by equally changing the triangle base angle—while keeping the loop length constant and equal to 2 wavelengths WL. In this way, the final antenna loop was shaped with 4 isosceles triangles. The analytical and simulated results for the radiation pattern were found to be in good agreement. Furthermore, a comparison with antenna's dipole counterpart characteristics showed a much better performance of the proposed antenna.

Keywords

Cross loop antenna, delta elements, analysis, simulation, improvement

Introduction

The cross loop antenna consisting of four delta elements was examined as a prototype antenna during preparation of an EECE diploma thesis [1]. The main available tools for its study were the antenna theory [2], the [RadPat4W] computer program

for antenna patterns [3] the [RICHWIRE] simulation program [4] and the mini-Suite of software tools [5]. Its simple plane figure of double symmetry with respect to two axes which means easy geometrical representation for the theoretical consideration of its radiation pattern as well

as for the simulation and easy construction, was the basic reason for this proposal. The initial antenna consists of four equilateral triangles with side length $\lambda/6$ and almost coincident their four vertices. Thus, the total length of the antenna is 2λ . The feed source was at the middle of the base of one of the triangles as it is shown in Fig. 1.

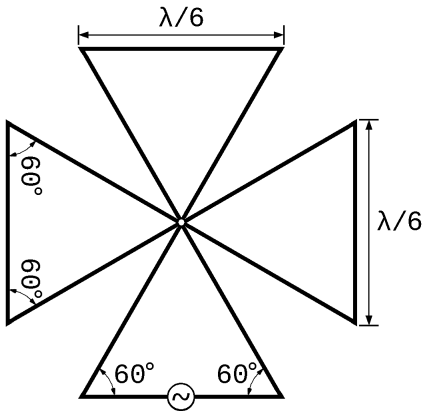


Fig. 1: Planar Delta-Cross Shaped Loop antenna

Then, the antenna was modified only with respect to the base angles of the triangles, keeping constant the triangle perimeter equal to $\lambda/2$, resulting a cross antenna of four isosceles triangles. The angle was varied between 48° and 78° , in order to improve both of its electrical and radiative characteristics and the one with

48° angle was selected as the improved Delta-Cross Shaped Loop antenna.

Analysis

The initial antenna was analytical studied considering standing waves, that is, sinusoidal, current distribution in a parallel wire transmission line. Since the perimeter of each equilateral triangle is $\lambda/2$, the total antenna length is equal to 2λ and it corresponds to a properly formed short circuited transmission line. However, the study was carried out in a $5\lambda/2$ piece of open circuited transmission line, formed properly as in Fig. 2, since the available formula of equation (1) concerns open circuited two parallel wired transmission lines

$$\dot{I}(\ell) = \dot{I} \sin(\beta(h - |\ell|)) \quad (1)$$

with

$$-h \leq \ell \leq +h \text{ where } h = \frac{5}{4}\lambda .$$

The above current distribution (1) was used to evaluate the radiation pattern of the antenna through the relations

$$\vec{E} = e^{i\beta R_{kr}} \text{PF} \begin{bmatrix} \ell_\theta \\ \ell_\varphi \end{bmatrix} \quad (2)$$

$$\text{PF} = \int_{\ell_A}^{\ell_T} \dot{I}(\ell) e^{i\beta \ell_r \ell} d\ell \quad (3)$$

According to the basic standing wave theory: i) the direction of current changes per $\lambda/2$ segment, ii) between two successive standing wave nodes the current phase remains the same and iii) if a source is between two successive standing waves the current direction does not change. These principles were applied at the properly bended 2-wire transmission line of Fig 2, keeping in mind that the Kirchhoff laws must be simultaneously satisfied.

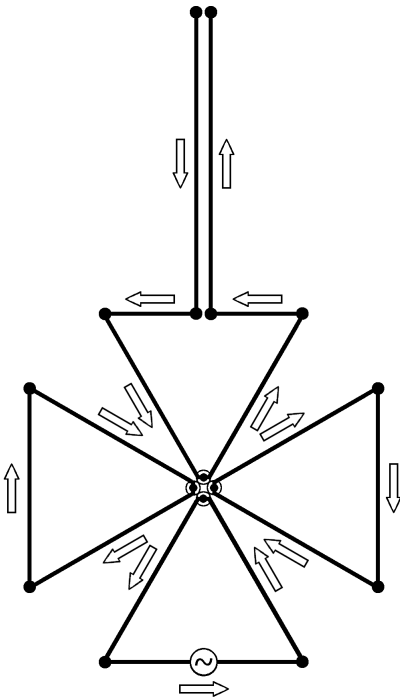


Fig. 2: $5\lambda/2$ properly bended 2-wire transmission line

The double arrows indicate the direction of $i\vec{\ell}$ product for every one segment, and the dotted circles at the almost coincident vertices of the four equilateral triangles correspond to a zero in the current distribution.

The two parallel $\lambda/4$ segments are almost coincident with opposite currents, so they are mutually canceled as for the radiation and they are excluded from further study. Thus, the remaining segments form the desired antenna, with total length 2λ and a current maximum at the source, as it is shown in Fig. 3.

For every one segment 0-12, of Fig. 3, we had to determine four quantities: the length of its starting point ℓ_A , the length of its end point ℓ_T , the position vector of its center \vec{R}_k , as if they were part of the corresponding line of 2λ length, and its unit direction vector $\vec{\ell}'_i$, with its direction to be in all segments from ℓ_A to ℓ_T . The planar antenna was arranged on yOz as it is shown in Fig. 4, along with all the \vec{R}_k position vectors as they were determined by the relation

$$\vec{R}_{k_v} = \vec{O}\vec{A}_v - \ell_{A_v} \vec{\ell}'_v \quad (4)$$

and Tab. 1 contains all the above mentioned geometrical quantities.

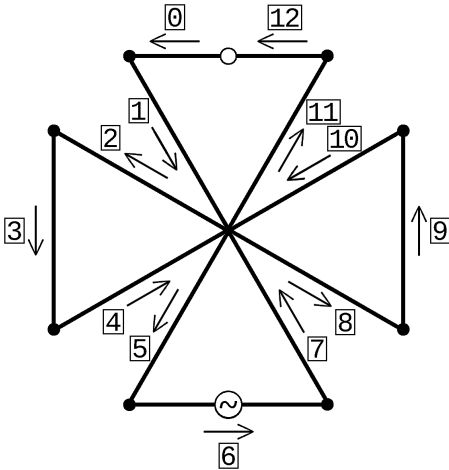


Fig. 3: 13 segments

Then through (1)-(3), that is, after the evaluation of the definite integral for the Pattern Factor PF [2], [6] the radiation pattern of all the 13 segments was formulated and according to the law of superposition the total radiation pattern is given by

$$\begin{aligned} \vec{E} &= \sum_{v=0}^{12} \begin{bmatrix} \dot{E}_{v\theta} \\ \dot{E}_{v\varphi} \end{bmatrix} = \begin{bmatrix} \dot{E}_{\theta} \\ \dot{E}_{\varphi} \end{bmatrix} = \dot{E}_{\theta_I} \vec{\theta}_I + \dot{E}_{\varphi_I} \vec{\varphi}_I = \\ &= (E_{\theta_R} + iE_{\theta_I}) \vec{\theta}_I + (E_{\varphi_R} + iE_{\varphi_I}) \vec{\varphi}_I \end{aligned} \quad (5)$$

which, after a lot of symbolic manipulation where the real parts are mutually eliminated, leads to a more simplified expression

$$\vec{E} = \begin{bmatrix} \dot{E}_{\theta} \\ \dot{E}_{\varphi} \end{bmatrix} = i (E_{\theta_I} \vec{\theta}_I + E_{\varphi_I} \vec{\varphi}_I) \quad (6)$$

and by the symmetry of the geometry radiation patterns of 0th, 12th and 6th wire are combined, as well as the five (5) couples: 1, 7 - 2, 8 - 3, 9 - 4, 10 and 5, 11 as it is obvious from Tab. 1. Thus, the total radiation pattern is

$$\begin{aligned} \vec{E} &= \vec{E}_{0,12,6} + \vec{E}_{1,7} + \vec{E}_{2,8} + \\ &+ \vec{E}_{3,9} + \vec{E}_{4,10} + \vec{E}_{5,11} \end{aligned} \quad (7)$$

Simulation

The simulation process was carried out in terms of [RICH-WIRE] program. The center frequency was 1111 [MHz] where the wavelength is $\lambda = 0.27$ [m] and the wire radius was 1 [mm]. We studied the antenna characteristics both electric and electromagnetic (SWR, Input Impedance, Directivity, Radiation Pattern) in the range [600, 1300] MHz around the center frequency with a 10 [MHz] step.

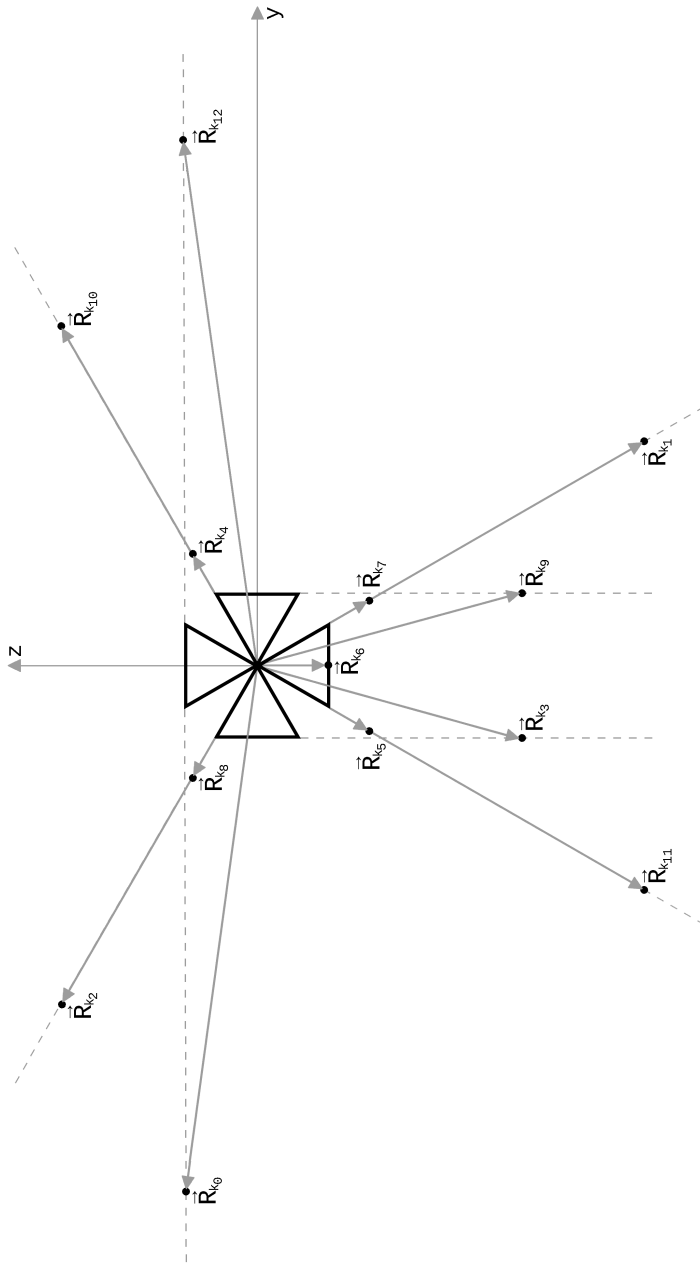


Fig. 4: 13 position vectors

Tab. 1: Geometrical Data

#	ℓ_A	ℓ_T	\vec{R}_k		βR_{k_r}
			\vec{y}_i	\vec{z}_i	
0	$-\lambda$	$-\frac{11}{12}\lambda$	$-\lambda$	$\frac{\sqrt{3}}{12}\lambda$	$-2\pi\sin\theta\sin\varphi + \frac{\sqrt{3}\pi}{6}\cos\theta$
1	$-\frac{11}{12}\lambda$	$-\frac{9}{12}\lambda$	$\frac{3}{8}\lambda$	$-\frac{3\sqrt{3}}{8}\lambda$	$\frac{3\pi}{4}\sin\theta\sin\varphi - \frac{3\sqrt{3}\pi}{4}\cos\theta$
2	$-\frac{9}{12}\lambda$	$-\frac{7}{12}\lambda$	$-\frac{3\sqrt{3}}{8}\lambda$	$\frac{3}{8}\lambda$	$-\frac{3\sqrt{3}\pi}{4}\sin\theta\sin\varphi + \frac{3\pi}{4}\cos\theta$
3	$-\frac{7}{12}\lambda$	$-\frac{5}{12}\lambda$	$-\frac{\sqrt{3}}{12}\lambda$	$-\frac{\lambda}{2}$	$-\frac{\sqrt{3}\pi}{6}\sin\theta\sin\varphi - \pi\cos\theta$
4	$-\frac{5}{12}\lambda$	$-\frac{3}{12}\lambda$	$\frac{\sqrt{3}}{8}\lambda$	$\frac{\lambda}{8}$	$\frac{\sqrt{3}\pi}{4}\sin\theta\sin\varphi + \frac{\pi}{4}\cos\theta$
5	$-\frac{3}{12}\lambda$	$-\frac{\lambda}{12}$	$-\frac{\lambda}{8}$	$-\frac{\sqrt{3}}{8}\lambda$	$-\frac{\pi}{4}\sin\theta\sin\varphi - \frac{\sqrt{3}\pi}{4}\cos\theta$
6	$-\frac{\lambda}{12}$	$\frac{\lambda}{12}$	0	$-\frac{\sqrt{3}}{12}\lambda$	$-\frac{\sqrt{3}\pi}{6}\cos\theta$
7	$\frac{\lambda}{12}$	$\frac{3}{12}\lambda$	$\frac{\lambda}{8}$	$-\frac{\sqrt{3}}{8}\lambda$	$\frac{\pi}{4}\sin\theta\sin\varphi - \frac{\sqrt{3}\pi}{4}\cos\theta$
8	$\frac{3}{12}\lambda$	$\frac{5}{12}\lambda$	$-\frac{\sqrt{3}}{8}\lambda$	$\frac{\lambda}{8}$	$-\frac{\sqrt{3}\pi}{4}\sin\theta\sin\varphi + \frac{\pi}{4}\cos\theta$
9	$\frac{5}{12}\lambda$	$\frac{7}{12}\lambda$	$\frac{\sqrt{3}}{12}\lambda$	$-\frac{\lambda}{2}$	$\frac{\sqrt{3}\pi}{6}\sin\theta\sin\varphi - \pi\cos\theta$
10	$\frac{7}{12}\lambda$	$\frac{9}{12}\lambda$	$\frac{3\sqrt{3}}{8}\lambda$	$\frac{3}{8}\lambda$	$\frac{3\sqrt{3}\pi}{4}\sin\theta\sin\varphi + \frac{3\pi}{4}\cos\theta$
11	$\frac{9}{12}\lambda$	$\frac{11}{12}\lambda$	$-\frac{3}{8}\lambda$	$-\frac{3\sqrt{3}}{8}\lambda$	$-\frac{3\pi}{4}\sin\theta\sin\varphi - \frac{3\sqrt{3}\pi}{4}\cos\theta$
12	$\frac{11}{12}\lambda$	λ	λ	$\frac{\sqrt{3}}{12}\lambda$	$2\pi\sin\theta\sin\varphi + \frac{\sqrt{3}\pi}{6}\cos\theta$

#	$\vec{\ell}_i$		ℓ_r	ℓ_θ	ℓ_ϕ
	\vec{y}_i	\vec{z}_i			
0	-1	0	$-\sin\theta\sin\varphi$	$-\cos\theta\sin\varphi$	$-\cos\varphi$
1	$\frac{1}{2}$	$-\frac{\sqrt{3}}{2}$	$\frac{1}{2}\sin\theta\sin\varphi - \frac{\sqrt{3}}{2}\cos\theta$	$\frac{1}{2}\cos\theta\sin\varphi + \frac{\sqrt{3}}{2}\sin\theta$	$\frac{1}{2}\cos\varphi$
2	$-\frac{\sqrt{3}}{2}$	$\frac{1}{2}$	$-\frac{\sqrt{3}}{2}\sin\theta\sin\varphi + \frac{1}{2}\cos\theta$	$-\frac{\sqrt{3}}{2}\cos\theta\sin\varphi - \frac{1}{2}\sin\theta$	$-\frac{\sqrt{3}}{2}\cos\varphi$
3	0	-1	$-\cos\theta$	$\sin\theta$	0
4	$\frac{\sqrt{3}}{2}$	$\frac{1}{2}$	$\frac{\sqrt{3}}{2}\sin\theta\sin\varphi + \frac{1}{2}\cos\theta$	$\frac{\sqrt{3}}{2}\cos\theta\sin\varphi - \frac{1}{2}\sin\theta$	$\frac{\sqrt{3}}{2}\cos\varphi$
5	$-\frac{1}{2}$	$-\frac{\sqrt{3}}{2}$	$-\frac{1}{2}\sin\theta\sin\varphi - \frac{\sqrt{3}}{2}\cos\theta$	$-\frac{1}{2}\cos\theta\sin\varphi + \frac{\sqrt{3}}{2}\sin\theta$	$-\frac{1}{2}\cos\varphi$
6	1	0	$\sin\theta\sin\varphi$	$\cos\theta\sin\varphi$	$\cos\varphi$
7	$-\frac{1}{2}$	$\frac{\sqrt{3}}{2}$	$-\frac{1}{2}\sin\theta\sin\varphi + \frac{\sqrt{3}}{2}\cos\theta$	$-\frac{1}{2}\cos\theta\sin\varphi - \frac{\sqrt{3}}{2}\sin\theta$	$-\frac{1}{2}\cos\varphi$
8	$\frac{\sqrt{3}}{2}$	$-\frac{1}{2}$	$\frac{\sqrt{3}}{2}\sin\theta\sin\varphi - \frac{1}{2}\cos\theta$	$\frac{\sqrt{3}}{2}\cos\theta\sin\varphi + \frac{1}{2}\sin\theta$	$\frac{\sqrt{3}}{2}\cos\varphi$
9	0	1	$\cos\theta$	$-\sin\theta$	0
10	$-\frac{\sqrt{3}}{2}$	$-\frac{1}{2}$	$-\frac{\sqrt{3}}{2}\sin\theta\sin\varphi - \frac{1}{2}\cos\theta$	$-\frac{\sqrt{3}}{2}\cos\theta\sin\varphi + \frac{1}{2}\sin\theta$	$-\frac{\sqrt{3}}{2}\cos\varphi$
11	$\frac{1}{2}$	$\frac{\sqrt{3}}{2}$	$\frac{1}{2}\sin\theta\sin\varphi + \frac{\sqrt{3}}{2}\cos\theta$	$\frac{1}{2}\cos\theta\sin\varphi - \frac{\sqrt{3}}{2}\sin\theta$	$\frac{1}{2}\cos\varphi$
12	-1	0	$-\sin\theta\sin\varphi$	$-\cos\theta\sin\varphi$	$-\cos\varphi$

The total number of 96 segments for the whole antenna, where all sides had equal number of points, was selected for the simulation, after the investigation for 13, 24, 48, 72, 96, 120, 144, 168, 192, 216, 240 segments. The above mentioned characteristics remained almost constant after this number of 96 segments. An appropriate computer program was developed in Fortran to create the input file with antenna geometry for [RICHWIRE].

A very good agreement between simulated and analyti-

cal produced radiation patterns is shown in Fig. 5 for the three main planes in 1111 [MHz], although there is a point for discussion here. A closer examination, after 7 years from the initial work [1], of what was really compared in Fig. 5, proved that the analytical patterns illustrated corresponds to rather an upper bound of the absolute radiation pattern since it results from the sum of the 13 absolute radiation patterns and not from the total absolute radiation pattern.

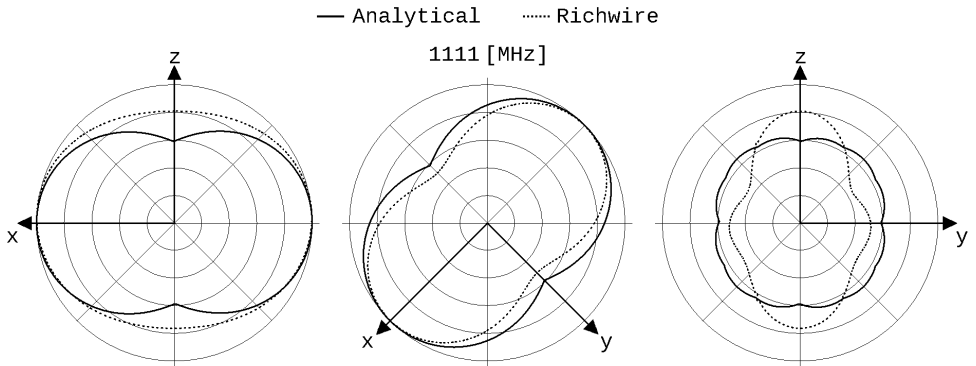


Fig. 5: Radiation patterns in 1111 [MHz]

Furthermore, the simulation model, as it is shown in Fig. 6, consists inevitable not in four equal delta elements but in four truncated ones, as care must be taken

- a) to avoid the overlapping of the wires in a future construction and
- b) to reduce the strong cou-

pling caused by the proximity effect.

Thus, the minimum permitted square region with side $(2a+a/10)$, where "a" is the used wire radius, was removed from the center intersection point of the four delta elements, while in the same time, in order to achieve the

connection of the neighboring sides, the base angles of every element are slightly greater than 60° , and the total length of such formed element was slightly greater than the initial $\lambda/2$.

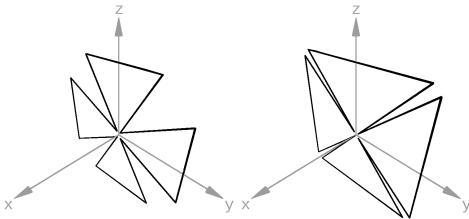


Fig. 6: Simulation models

Extremely high values of Standing Wave Ratio [SWR] in 1111 [MHz] for the three characteristic impedances 50, 75 and 300 $[\Omega]$ as it is shown

in Fig. 7, made clear the need for further research on the antenna's geometry.

The antenna was modified only with respect to the base angles for constant delta-perimeter, resulting a Delta-cross Loop antenna of four isosceles triangles. A computer program was also developed in Fortran producing the corresponding input data for [RICHWIRE].

The investigation was performed from the value of 48° for the base angles to 78° in step of 1° at the frequency of 1111 [MHz]. The best performance was noticed between 48° and 52° and the model, shown in Fig. 8, with 48° base angles was selected.

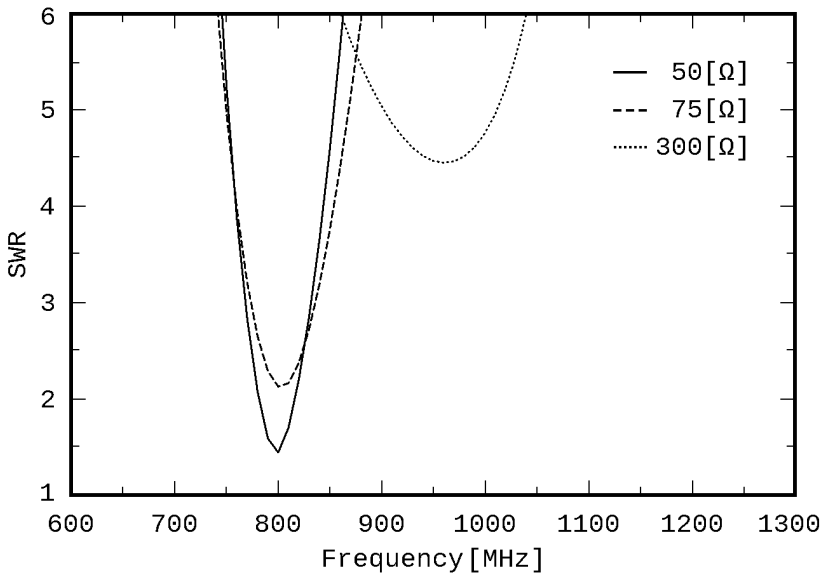


Fig. 7: Standing Wave Ratio against frequency

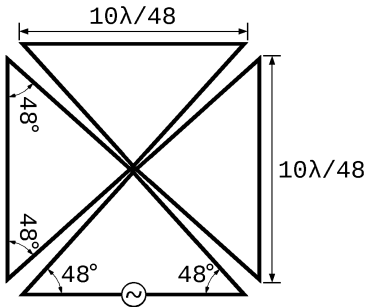


Fig. 8: Improved antenna

In Figs. 9 - 13 SWR, Input Impedance [Z_{in}] as Input Resistance R_{in} and Input Reactance X_{in} in [Ω] and Directivity D in [dB] of the improved antenna together with that of the initial one and of 2λ dipole, are shown respectively. Fig. 12 shows a properly selected window of the total frequency range for the Input Impedance in order to clarify the improvement of the modified antenna. In Figs. 14 - 15 a comparison of the radiation patterns of the three antennas is given at five frequencies in the three main planes zOx , xOy and yOz . In Fig. 16 the 3D analytical radiation pattern at 1111 [MHz] and in Fig. 17 the corresponding 3D patterns in all frequencies are shown.

Conclusion

Although, the agreement of results between simulation and analysis was very good,

the characteristics of the initial antenna were not satisfactory. An improvement process was needed and the research was here limited to the change of the base angles only to the rather small range of -12° , $+18^\circ$ around the initial 60° base angle. Thus, the improved antenna had the best performance about 100 MHz lower of the desired frequency of 1111 [MHz], as it is shown in Figs. 9 - 13. The SWR for the 50 [Ω] characteristic impedance has its best value closer to 1111 [MHz] while the initial antenna and the 2λ dipole of equivalent length had a relative small value of SWR at about 800 [MHz] (Fig. 9). It is also obvious that the Input Impedance as well as Directivity is relatively stable and slightly better for the improved antenna and much better from the initial one (Figs. 10 - 13). Corresponding values for SWR, Input Impedance and Directivity for the three antennas are given in Tab. 2.

The radiation pattern of the improved antenna is closer to that of a centered fed sinusoidal $\lambda/2$ dipole, avoiding the dispersion of radiation in multiple directions of the rather long 2λ dipole antenna (Figs. 14 - 15, 17).

Tab. 1: SWR, D, Z_{inp}

	SWR	D [dB]	Z_{inp} [Ω]
1111 [MHz]			
60°	43.7	2.49	40 - i 287
2 λ	26.1	4.09	577 - i 647
48°	6.55	3.10	70 + i 127
800 [MHz]			
60°	1.44	2.61	36 + i 5
2 λ	2.55	3.21	88 - i 52
48°	42.7	2.30	24 - i 219
1010 [MHz]			
60°	29.6	2.85	1297 + i 485
2 λ	20.4	3.74	993 + i 168
48°	1.26	2.90	40 + i 3

An extensive investigation concerning the analytical determination of the antenna radiation pattern and its normalized absolute values is in the immediate future plans of the authors in order to achieve the clarification of its relation with the one produced by simulation.

A wider range of the base angle variation or the variation of the total length of each delta element are some design ideas for a future research work. Nevertheless, the final step is, without doubt, the construction and measurement of the proposed antenna together with the comparison of the corresponding results.

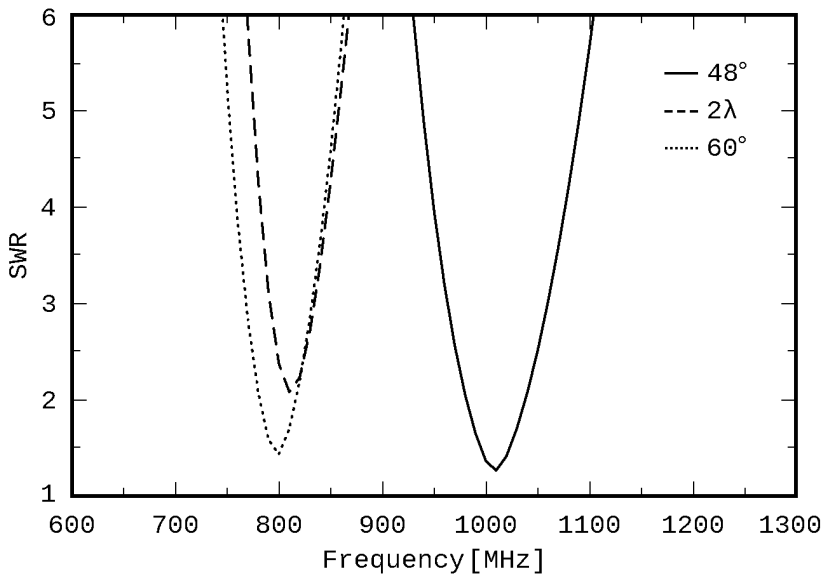


Fig. 9: SWR for improved-48°, 2 λ and initial-60° antenna

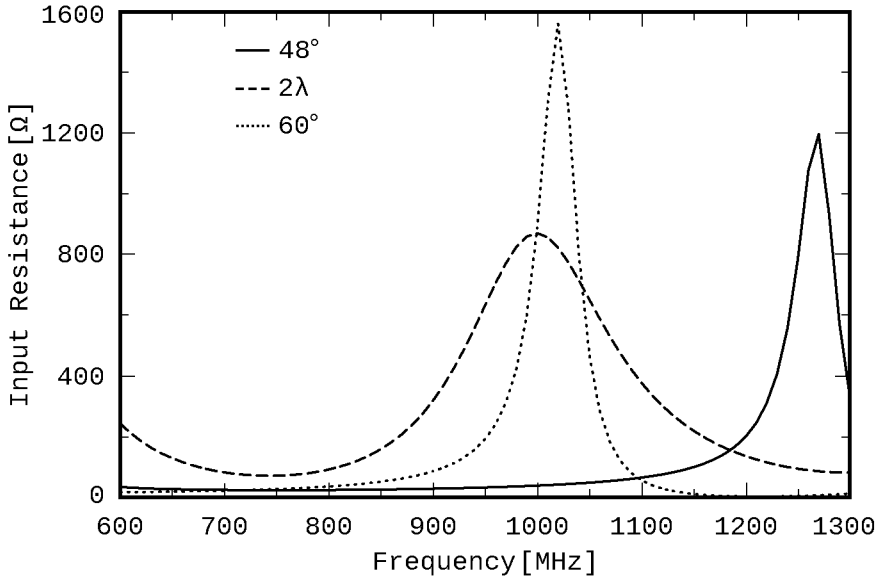


Fig. 10: R_{inp} for improved-48°, 2λ and initial-60° antenna

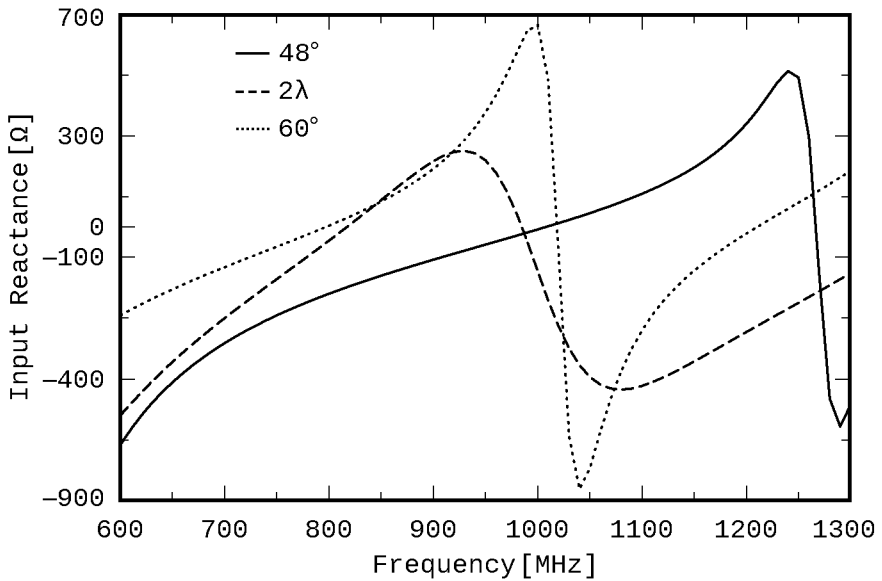


Fig. 11: X_{inp} for improved-48°, 2λ and initial-60° antenna

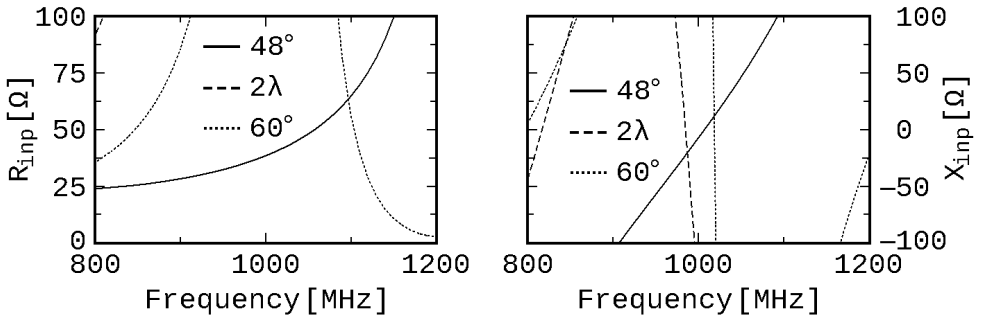


Fig. 12: R_{in} , X_{in} for the three antennas in [800, 1200] MHz

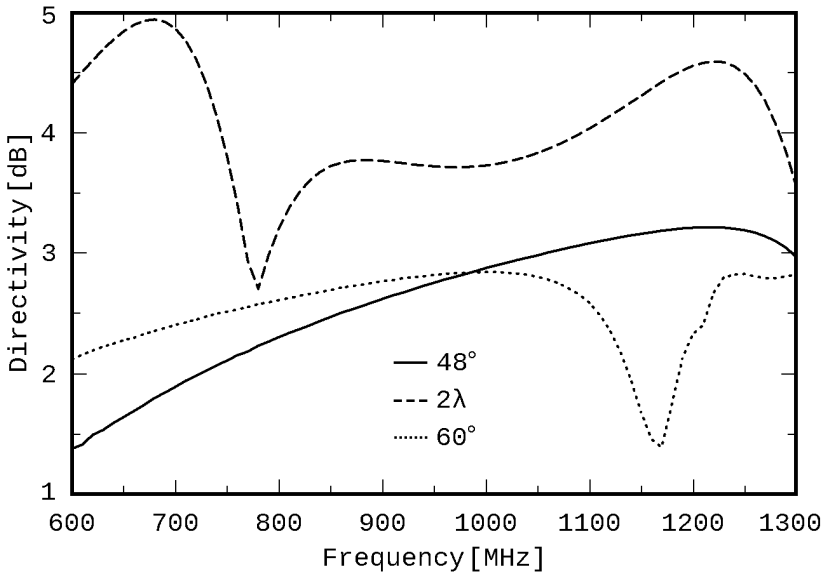


Fig. 13: Directivity of the three antennas

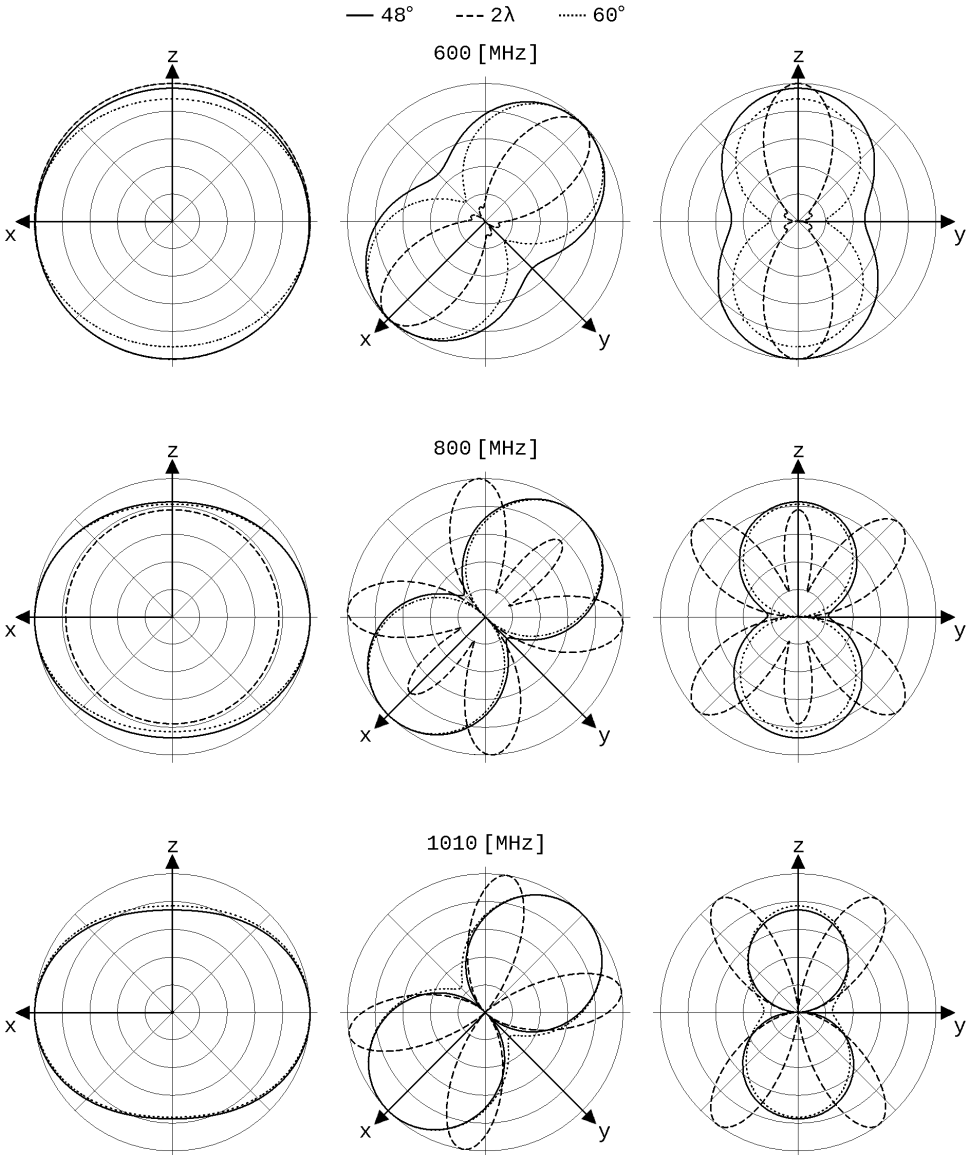


Fig. 14: Radiation patterns at 600, 800 and 1010 [MHz]

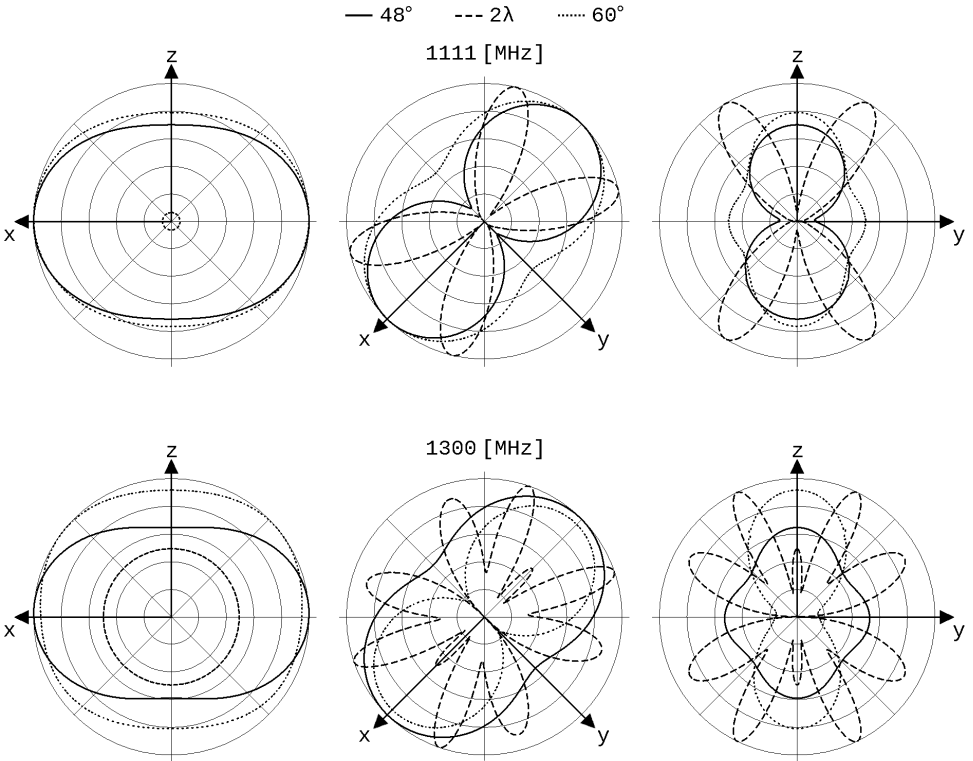


Fig. 15: Radiation patterns at 1111 and 1300 [MHz]

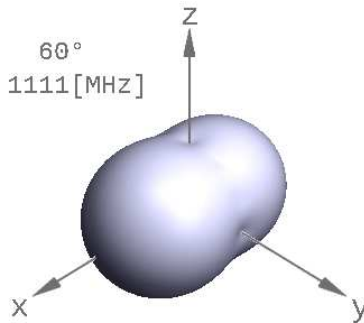


Fig. 16: 3D Analytical Radiation Pattern

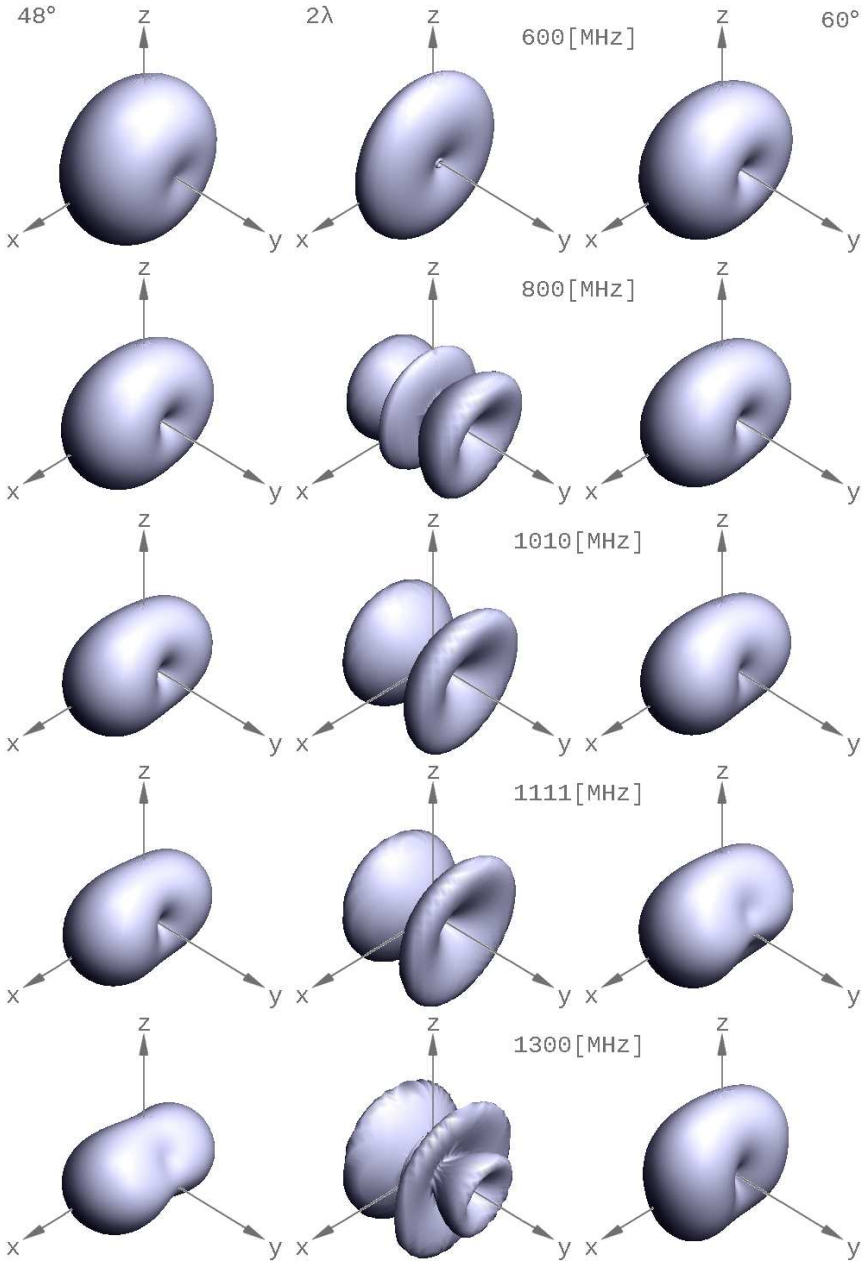


Fig. 17: 3D Simulated Radiation Patterns

References

- [1] Papadaniel G., "The Eisernes Kreuz Antenna [Prototype ARG-06]", Diploma Thesis #40, ARG-Antennas Research Group, DUTH, 2007 (in Greek)
- [2] Zimourtopoulos P., "Antenna Notes 1999-, Antenna Design Notes 2000-, <http://www.antennas.gr/antennanotes/> (in Greek)
- [3] Yannopoulou N., Zimourtopoulos P., "A FLOSS Tool for Antenna Radiation Patterns", Proceedings of 15th Conference on Microwave Techniques, COMITE 2010, Brno, Czech Republic, pp. 59-62
- [4] Richmond J.H., "Computer program for thin-wire structures in a homogeneous conducting medium", Publication Year: 1974, NTRS-Report/Patent Number: NASA-CR-2399, ESL-2902-12, DocumentID: 19740020595, <http://ntrs.nasa.gov/>
- [5] Yannopoulou N., Zimourtopoulos P., "Mini Suite of Antenna Tools, Educational Laboratories, Antennas Research Group, 2006, <http://www.antennas.gr/antsoft/minisuiteoftools/>
- [6] Yannopoulou N.I., "Study of monopole antennas over a multi-frequency decoupling cylinder", PhD Thesis, EECE, DUTH, February 2008 (in Greek), pp. (2-6)-(2-9)

*Active Links: 27.05.2015

Follow-Up Research Paper

Not until now

Previous Publication in FUNKTECHNIKPLUS # JOURNAL

"Visual EM Simulator for 3D Antennas: VEMSA3D – FLOSS for MS Windows", Issue 6, Year 2, pp. 7-25

* About The Authors

Nikolitsa Yannopoulou, Issue 1, Year 1, p. 15

Petros Zimourtopoulos, Issue 1, Year 1, p. 15

Papadaniel Glykeria, was born in Rodolivos-Amfipolis, Serres, Greece in 1981. She graduated from Electrical Engineering and Computer Engineering in 2007 from Democritus University of Thrace, Xanthi, Greece. Member of Antennas Research Group while she was elaborated her diploma thesis. She did practice exercise in the Hellenic Telecommunication Organisation and she worked as an Engineer in Clima, Voltampere Energy and Rodax Companies for the study/design of Photovoltaic systems, wind farms, natural gas plants and electrical installations in a thermoelectric power station. She is a certified three-dimensional graphics and computer aided Designer.

g.papadaniel@yahoo.gr